# Informing the Design of Novel Input Methods with Muscle Coactivation Clustering



MYROSLAV BACHYNSKYI, Max Planck Institute for Informatics and Saarland University
GREGORIO PALMAS, Max Planck Institute for Informatics
ANTTI OULASVIRTA, Max Planck Institute for Informatics and Saarland University
TINO WEINKAUF, Max Planck Institute for Informatics

This article presents a novel summarization of biomechanical and performance data for user interface designers. Previously, there was no simple way for designers to predict how the location, direction, velocity, precision, or amplitude of users' movement affects performance and fatigue. We cluster muscle coactivation data from a 3D pointing task covering the whole reachable space of the arm. We identify 11 clusters of pointing movements with distinct muscular, spatio-temporal, and performance properties. We discuss their use as heuristics when designing for 3D pointing.

Categories and Subject Descriptors: H.5.2 [**Information Interfaces and Presentation (e.g., HCI)**]: User Interfaces—*Ergonomics*

General Terms: Human factors, Performance, Design

Additional Key Words and Phrases: Muscle coactivation clustering, user interface design, physical ergonomics, user performance, biomechanical simulation

**ACM Reference Format:**
Myroslav Bachynskyi, Gregorio Palmas, Antti Oulasvirta, and Tino Weinkauf. 2015. Informing the design of novel input methods with muscle coactivation clustering. ACM Trans. Comput.-Hum. Interact. 21, 6, Article 30 (January 2015), 25 pages.
DOI: http://dx.doi.org/10.1145/2687921

## 1. INTRODUCTION

This article investigates a novel data-driven approach to biomechanical simulation to inform User Interface (UI) design. *Motion capture-based biomechanical simulation* is an inverse approach to observed motion of the human body. It bears great potential for Human-Computer Interaction (HCI) because it yields a very rich description of a user's movement—including velocities and angles of limb segments, forces and moments at joints, and, most importantly, muscle activations [Thelen et al. 2003]. Muscle activations could be particularly useful in interface design as indices of users' fatigue

This research was funded by the Cluster of Excellence for Multimodal Computing and Interaction at Saarland University, as well as the Max Planck Center for Visual Computing and Communication and the International Max Planck Research School for Computer Science at the Max Planck Institute for Informatics.
Authors' addresses: M. Bachynskyi, Cluster of Excellence MMCI, Saarland University Campus E 1.7 (Room 2.02), 66123, Saarbrücken, Germany; email: mbachyns@mpi-inf.mpg.de; G. Palmas, Max Planck Institute for Informatics, Saarland University Campus E 1.4 (Room 204), 66123, Saarbrucken, Germany; email: gpalmas@mpi-inf.mpg.de; A. Oulasvirta, School of Electrical Engineering, Aalto University, Otakaari 5, 13000, Aalto University, Finland; email: antti.oulasvirta@aalto.fi; T. Weinkauf, Max Planck Institute for Informatics, Saarland University Campus E 1.4 (Room 205), 66123, Saarbrucken, Germany; email: weinkauf@mpi-inf.mpg.de.

DOI: http://dx.doi.org/10.1145/2687921

and energy usage. Moreover, as a method, it has advantages over direct measurements like electromyography (EMG): It is nonintrusive; can estimate activation of all muscles, not only those close to surface; and it does not suffer from cross-talk, variable skin-conductivity, or muscle movement noise. Moreover, open simulation software is emerging [Delp et al. 2007], and optical motion tracking equipment is becoming more common in HCI laboratories around the world. However, despite the attempts to validate the method [Lund et al. 2012; Bachynskyi et al. 2014] and develop software [Delp et al. 2007; Rasmussen et al. 2002; Veloso et al. 2006; Murai et al. 2010], we have yet to see a breakthrough comparable to its success in medicine, industrial ergonomics, and sports perhaps because of the high costs of experimental setups and analyses.

Our goal is to make biomechanical simulation more accessible by significantly lowering the barriers to its use. To this end, we have investigated a way to *summarize the major muscle activations and user performance in interactive tasks*. As a concrete case, we investigate interfaces operated by pointing with the human arm. Aimed movements [MacKenzie 1992] are ubiquitous in HCI and typically registered by intermediaries such as mouse, touchpad, trackpoint, or joystick. In-air pointing with the arm has recently become more important with the development of advanced computer vision methods and other sensors. Recent examples of freehand pointing and gesturing include medical image exploration [Gallo et al. 2011], tabletops [Wobbrock et al. 2009], hand articulation interactions [Chaudhary et al. 2013], large interactive displays [Vogel and Balakrishnan 2005; Banerjee 2012], projector phones [Winkler et al. 2012], video gaming, exergames [Sinclair et al. 2007], and rehabilitation [Lange et al. 2011].

We propose a *clustering* that summarizes the main aspects of pointing movements with the human arm from a biological perspective and associates them with standard measurements of user performance. Associating muscle loading with performance data is useful for HCI because a usable input method not only allows the user to send a high rate of "messages" with movement, but it also minimizes physical ergonomic costs such as energy use, muscular load, fatigue, and strain.

Formally, *clusters* refer to "patterns whose distribution in feature space is governed by a probability density specific to each cluster" [Jain et al. 1999: 7]. In our particular case, the clusters are understood as *muscular equivalence sets* of aimed movements that are similar in time-dependent muscle coactivation patterns in an upper extremity of the human body. The clustering concerns the time-dependent activation signal of 41 muscles of the upper extremities in pointing movements. Every movement in this dataset is mapped to one cluster for which we also compute standard indices of performance (speed, accuracy, throughput) from the optical tracking data. The clustering is based on a novel dataset in which muscle coactivations are estimated for real 3D pointing performance of an athlete uniformly covering *the whole reachable space* of the arm: altogether 72,000 movements. To our knowledge, this is the most comprehensive dataset of this kind; as we explain later, it covers many scenarios of novel user UIs.

The clusters capture the largest trends in the highly *nonuniform* motion space of the human arm. Previous work has demonstrated that the space of pointing movements in general is nonuniform with respect to location [Caminiti et al. 1990], direction [Caminiti et al. 1991], performance [Hoffmann et al. 2011; Grossman and Balakrishnan 2004; Lin and Ho 2011; Plamondon and Alimi 1997; Harris and Wolpert 1998; Whisenand and Emurian 1999], and involved muscles [Koshland and Hasan 1994]. Because muscles differ in size, fiber distribution, and force-length-velocity properties, they are differentially recruited in movements in terms of force, timing, moment, and acceleration. A movement of the arm on the left-hand side of the torso will recruit a different subset of muscles than will a movement on the right-hand side. We sought to find a minimum number of clusters that captures such variability in the whole reachable space of the arm.

The clustering makes the assumption that muscles are mainly responsible for the physical forces behind a movement. Human movements are produced by neural impulses (action potential) transferred by the neural system to muscles, similarly to electric current. Muscles react to action potential by contraction to produce an active force. Forces produced by groups of muscles working at a particular joint sum to produce total moment at the joint. Finally, the joint rotates, producing visible movement. In this regard, their activation patterns contain the necessary "information" about movement. Thus, our clustering task makes no prior assumption that certain locations, directions, or amplitudes of movements are "special," but it lets such differences emerge bottom-up from muscle coactivations. Moreover, the idea of clustering coactivation patterns is biologically plausible in the light of a current theory of how muscles act together synergistically [Tresch et al. 1999]. However, our clustering is a bottom-up summarization of muscle simulation data and is meant for practical purposes in HCI rather than taken as a neuromechanical hypothesis. Biomechanical simulation subscribes to the assumption that the neural system is optimal in that it produces ideal (optimal) activation signals and transmits them losslessly to muscles. Thus, the clusters are best viewed as a summarization of the upper boundary of human pointing performance in the absence of moderating neural (e.g., signal loss), muscular (e.g., suboptimal muscle recruitment), or physical (e.g., friction) factors. We also show that predictive models of movement time can be improved based on the clusters.

This article builds on previous work from HCI and motor control and broadens it by:

—collecting an extensive dataset of aimed movements uniformly covering the whole space reachable by the arm,
—augmenting the dataset with activation data of all the main muscles of the upper extremity, including those not accessible by previous analysis methods,
—associating pointing performance, location in 3D space, and ergonomics properties of movements with muscle activation patterns,
—summarizing a complex dataset with multisource data in a single simple-to-understand clustering.

The clustering can be be utilized by practitioners as a *heuristic* prior to or in the absence of a full-fledged biomechanical analysis. The clusters predict the performance and muscle loading of a given pointing gesture with location, direction, and amplitude. As we show, a whole *input region* can be defined consisting of a set of movements that a designer expects for a given user interface. It can also be used inversely: Given target ranges for muscle loads and user performance, the permissible movements can be identified. Thus, instead of working with separate movement models and biomechanics methods, designers can cross-check the demands of a movement if they know anything about its ego-centric location. The clustering may help designers in four pursuits:

(1) Assess if a given input style is efficient or if slight changes could improve it
(2) Compare different input styles
(3) Identify input regions with optimal tradeoffs between performance and muscle load
(4) Find ways to alternate between muscle groups that can minimize fatigue

We conclude with a demonstration of applications in HCI and discuss opportunities in using optical motion tracking-based biomechanical simulation in HCI more broadly. Although this article focuses on the case of interfaces controlled with large arm movements, the approach followed here will have broader usability once the tracking and simulation techniques allow us to deal with dynamic ground reaction forces (e.g., upon touching a display) and fine motor movements involving the fingers [Vignais et al. 2013].

## 2. RELATED WORK

There is compelling evidence suggesting nonuniformity of human movement: two movements that differ in location, direction, and amplitude can and will vary in many important aspects. Simplifying these heterogeneous patterns is the prime goal of our work.

First, *studies of movement trajectories* have shown the tangential velocity pattern generally to be asymmetric and bell-shaped [Freund and Büdingen 1978]. However, several factors affect trajectory and velocity profiles, such as starting posture, the location of the end-effector, and ending posture [Soechting et al. 1995], as well as the availability of visual feedback [Adamovich et al. 1999; Gribble et al. 2003; Baud-Bovy and Viviani 1998]. Movement properties also depend on ego-centric location and direction of movement [Caminiti et al. 1990, 1991; Koshland and Hasan 1994]. Some of these effects have been captured in a number of movement models, including the minimum jerk principle [Todorov and Jordan 1998], the torque change minimization model [Uno et al. 1989], and the endpoint variance minimization model [Harris and Wolpert 1998]. Our experimental paradigm for data collection includes the effects of different starting postures, egocentric location, and direction. No limitations were imposed on the use of visual feedback.

Second, *performance models* capture the speed-accuracy tradeoff of pointing tasks [Hoffmann et al. 2011; Grossman and Balakrishnan 2004; Lin and Ho 2011; Plamondon and Alimi 1997; Harris and Wolpert 1998]. The earlier models treated movements as equal in regards to starting location and direction [Fitts 1954; Welford 1968; Schmidt et al. 1979; MacKenzie and Buxton 1992; MacKenzie 1992]. Some recent models have started to capture these factors [Grossman and Balakrishnan 2004; Plamondon and Alimi 1997; Cha and Myung 2013]. Because three target sizes were used and the whole 3D space of the arm covered, our dataset allows grouping any movements in the 3D space for performance modeling. The clusters we identify differ in movement location, direction, and amplitude. We show that performance prediction can be improved by segmenting the data based on muscle-based clusters.

Third, *studies of muscle dynamics* have shown a general three-phasic pattern of muscle activations from agonist to antagonist [Wierzbicka et al. 1986; Gielen et al. 1985]. Muscle activations in the initial agonist activation are directly proportional to the duration of the acceleration phase [Cooke and Brown 1994; Wadman et al. 1979]. Durations of the initial electromyelogram (EMG) bursts of the agonist muscles are proportional to the movement amplitude [Gielen et al. 1985]. It has been found that the set of muscles activated at the initialization phase of movement depends on the target location [Koshland and Hasan 1994]. Also, depending on the movement direction, a common waveform of muscle activation is scaled and delayed in a specific way for each muscle [Flanders 1991]. Furthermore, earlier studies have exposed co-dependencies, such that shoulder and elbow joints are coupled during movement, but the wrist is independent [Lacquaniti et al. 1986; Hong et al. 1994]. Our muscle activation data confirm the general pattern and, as such, show large differences within the pointing space (see Section 3). The goal of our clustering is to capture the tendencies in the whole reachable space of the arm. As stated, no a priori assumptions are made about muscle recruitment, but we identify classes in a data-driven approach.

We are aware of few attempts to apply statistical methods of modeling, classifying, or clustering to biomechanical data. Santos et al. performed clustering of kinetic and kinematic variables of gait and stair ascent and descent to identify different functional fitness levels of elderly people [Santos et al. 2014]. However, this work was focused on identification of the most relevant feature set and used ground truth data identified in a separate test to assess quality of clustering. Even fewer papers attempt to model and classify muscle activation patterns of arm movements. They are based on EMG recordings that were statistically related to kinematics or dynamics of the arm.

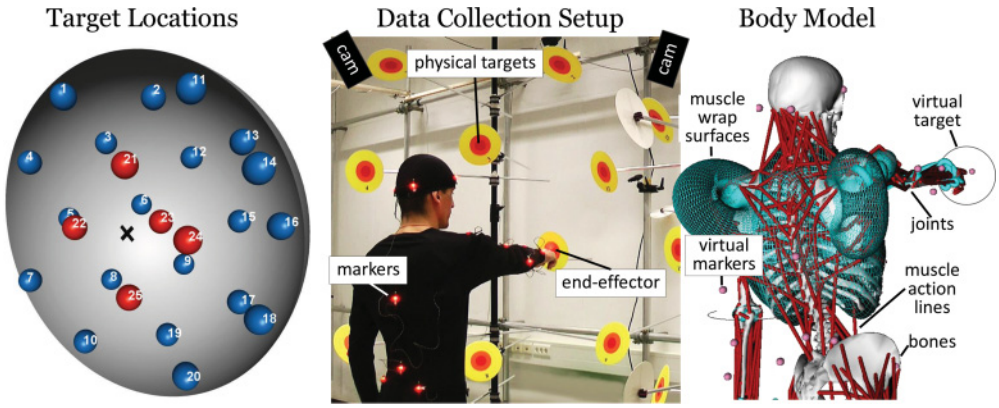


Fig. 1. Performance was recorded for all reciprocal pointings among 25 targets (left) covering the reachable space of the arm. To allow biomechanical simulation, optical markers on the subject's body (center) are mapped via anatomical landmarks to a generalized model of the human (right). Physical targets are registered in the virtual 3D space to allow the computation of performance metrics (speed, accuracy, and throughput).

Flanders [1991] extracts two principal components from the EMG signals. These components contain similar patterns among muscles, with the differences in amplitude and temporal shift depending on the desired movement direction. Micera et al. [1999, 2000] use machine learning techniques to classify EMG signals into three categories. The involved movements are all planar, and only three muscles are examined. These studies account for nonuniformity, but they cover only a narrow set of upper extremity muscles and are limited to close-to-the-surface muscles. Moreover, they do not associate the patterns to pointing performance.

In our previous work, we collected the motion capture dataset of aimed movements [Bachynskyi et al. 2013] covering the whole reachable space. We validated biomechanical simulation for the full-arm aimed movements [Bachynskyi et al. 2014]. To better support visual analysis of complex datasets consisting of spatial, performance, and ergonomic variables, we developed an interactive visualization tool [Palmas et al. 2014]. This background allows us to build on previous work on modeling movement data by

—including the main muscles of the upper extremities,
—covering the whole reachable space of the arm,
—associating activation patterns to pointing performance.

## 3. DATA COLLECTION

To cover all aimed movements within the reachable space of the arm, we collected optical motion tracking data of the 3D pointing performance of an athlete. The dataset contains 72,000 movements among 25 targets uniformly covering the whole reachable space of the dominant arm.

We tracked the full-body motion of the subject during the movements. Motion capture data of the full body allows us to perform biomechanical simulation of recorded movements to look at the indices inside the body: joint angles, moments and forces at joints, forces exerted by muscles, and muscle activations [Delp et al. 2007]. These data can be also used as an estimation of energy expenditure and fatigue indices for each movement.

The data collection setup with the 25 targets is shown at the left in Figure 1. Since we use targets with three different sizes (yellow, orange, and red in the figure) and include

varying target-to-target distances, the data allow for the computation of performance models.

The athlete is an amateur kickboxer: This sport emphasizes stamina and hand-eye coordination. Hence, the dataset estimates the upper bound of performance reachable by regular users. By studying aimed movements to *physical targets* with no intermediary input device, we can study the performance directly without the typical limitations of devices such as dwell-time, visibility of the user interface, or latency of cursor updates.

### 3.1. Method

**Participant:** The subject is a 27-year-old male (right-handed, 180cm, 72.5kg) with no known health problems. During the past 5 years, he placed first in the French and German amateur kickboxing competitions. However, he is a well-balanced athlete and regularly does different types of training in addition to kickboxing: athletics and running, push-ups and pull-ups, cycling, swimming, hiking, and dancing.

**Movement targets:** Figure 1 (left) shows the reachable space studied: a half-sphere with radius equal to the subject's arm length and centered at the right shoulder's pivot point. The targets were distributed over the 3D space by means of the densest sphere-packing algorithm. They were created from cardboard disks of three colors (yellow, orange, and red) that correspond to three target-width conditions, with radii of 8cm, 4cm, and 2cm, respectively. These were attached to the ends of aluminum pipes. To ensure that the shoulder stays at the center of the sphere, we prevented leaning with a horizontal obstacle placed about 2 cm in front of the chest.

**Experimental design:** The experiment consists of 80–85 aiming movements carried out for all pairs of the 25 targets, each with three target-width conditions (2, 4, and 8cm). This yields a total of 72,000 pointing acts. The order of trials was randomized in the experiment.

**Procedure:** Thirty sessions of 90–120 minutes each were carried out over three weeks. The subject stands in a position marked on the floor and repeatedly moves between two given targets as accurately and quickly as possible. Before each target pair, the subject can find the best manner of aiming at the targets. Timing starts with the index finger on a target. After a trial, if the self-reported fatigue level is high, 5 minutes of rest is allowed. All movements were made with the subject's dominant hand. We imposed a minimum recovery interval of 6 hours between sessions to allow fast twitch muscle fibers to restore their potential energy.

**Apparatus:** The *PhaseSpace* system with 12 Impulse cameras at 480fps was used to record the movement of 38 active markers (Figure 1, center). Marker placement was done with care to minimize drift during a session. The tracking accuracy is approx. 1/5 mm.

### 3.2. Performance Indices and Modeling

We computed movement speed and offset to the target center (inaccuracy) as indices of pointing performance. The *effective target width* $W_e$ was computed as a width of a sphere containing 96% of movement endpoints at the target [MacKenzie 1992]. The *movement time* ($MT$) is the time necessary for the participant to move from the starting point to the target, and, for each condition of target pair and target size, we calculate the $MT$ value as the average time length of all corresponding movements recorded in the experiment. *Indices of difficulty* (*ID*s) and Fitts's law models of $MT$ were calculated for a set of amplitudes $D$ and target sizes $W_e$ of movements belonging to a particular

cluster as

$$ID = \log_2(D/W_e + 1)$$
$$MT = a + b \times ID,$$

where $a$ and $b$ are regression coefficients of a linear model fit for the given set of movements. To check goodness of fit for each model, we computed the coefficient of determination $R^2$.[1]

### 3.3. Biomechanical Simulation

Optical motion capture provides only a cloud of points in 3D space tracked on the body during the movement. The biomechanical simulation is necessary to transform that cloud of points to the space of indices describing the processes inside the body; among them, muscle activations are of particular interest for the HCI analyses.

Currently, the best-known software tools for biomechanical simulation are OpenSim, AnyBody, LifeModeler, and SantosHuman. We chose *OpenSim* [Delp et al. 2007], the only comprehensive open source simulator. It supports editing of the musculoskeletal model, scripting, and visual investigation of the results in a GUI. Because of the lack of free high-fidelity full-body models, we use the commercial *SIMM Full Body model* (SIMM-FBM). SIMM-FBM combines measurements from several anatomical studies [Holzbaur et al. 2005; Delp et al. 2001; Vasavada et al. 1998; de Leva 1996]. It contains models of 118 bones, 86 joints, and 285 muscles. The measurements represent an average adult male and must be scaled to the actual subject before simulation. An example is shown in Figure 1 (right).

The following steps are standard parts of the pipeline. We report the basic idea of each step with necessary modifications:

**1. Mapping:** The first step is to find a correspondence between model and pointlights in the 3D mocap data. A *virtual marker set* must be defined, associating physical marker positions with positions in the musculoskeletal model. We follow the standards and guidelines for marker placements for biomechanical analysis [Kontaxis et al. 2009].

**2. Scaling** of the musculoskeletal model to a subject's proportions is then performed. *A measurement set* is a set of marker pairs and body parts that are scaled according to the ratio of distances between virtual and physical markers. The model size and weight are adjusted on the basis of the measurement set or from manual measurements.

**3. Marker adjustment** is done by means of Inverse Kinematics (IK) for a calibration dataset, with adjustment of marker positions to minimize errors between virtual and physical markers.

**4. IK** [Delp et al. 2007] calculates generalized coordinates that describe skeletal movement. The output is angles between bones at joints and translations and rotations of bodies in the human model relative to the ground. IK is calculated by an optimizer that minimizes weighted least-squares errors between physical markers and corresponding virtual markers.

**5. Inverse Dynamics** [Delp et al. 2007] (ID) calculates *forces and moments at joints* produced by movement stored in a generalized-coordinate sequence. External forces can be added to the simulation at this step (e.g., if recorded by force plate, force transducers, or dynamometers).

**6. Static Optimization** [Delp et al. 2007] (SO) resolves the required *activations of muscles* by minimizing *total* muscle activation as its objective function. It uses two

[1]We currently use a univariate model of pointing because model fit is good enough, but bivariate and trivariate models can be computed based on these data (e.g., Grossman and Balakrishnan [2004]).

muscle models as constraints: ideal force generators and muscles constrained by force-length-velocity properties. Because of computational demands, SO was performed for a selected set of 1,800 movements. One *representative movement* was selected for each target pair ($25 \times 24$) and size (3) on the basis of accuracy and proximity to mean speed.[2]

### 3.4. Validation

Because our analysis is based on a single participant, a trained athlete, we wanted to confirm that his movements do not differ significantly from those of "regular users." The fact that the participant performs balanced training in different sports is very important here because he trains not only some particular muscle, but all muscles of his body uniformly. Hence, his muscles are proportionally more powerful than the muscles of a regular person, but he recruits them in a very similar way. To this end, we acquired a recently published dataset that used exactly the same experimental setup and task with 16 participants (9 m, 7 f, mean age 26, mean height 170cm, mean weight 70kg) [Bachynskyi et al. 2014]. The task is otherwise the same, but a stratified sample of five targets was used per subject (the athlete dataset has 25 targets).

To compare movement style between the athlete and the 16 participants, we computed correlations for marker positions, movement velocity, joint angles, and moments. The obtained correlations show that although the athlete was much faster at the task, the movement style was very similar: absolute position ($r = 0.98$), absolute velocity ($r = 0.97$), joint angles ($r = 0.87$), and joint moments ($r = 0.75$).

## 4. OVERVIEW OF THE DATASET

The obtained dataset provides a rich description of human movement when pointing in 3D. It contains more than 400 variables describing complex interrelations between spatial locations, performance, and ergonomics:

—**spatial information:** 28 variables including target positions and sizes, trajectories of the end-effector, velocity, acceleration, directionality in polar coordinates, and angles of projections on two vertical planes and with origin at the shoulder center;
—**performance:** 17 variables including accuracy, movement time, effective target width, index of difficulty, Fitts's law model parameters and coefficient of determination, throughput;
—**ergonomics:** 361 variables including moments and forces for 21 joints, and forces and activations for 41 muscles per frame, as well as corresponding aggregated values for complete movements.

We briefly present an overview of the dataset here before proceeding to the clustering method in the next section. A table with a full dataset description is available as supplementary material.

Figure 2 shows the nonuniformity of aimed movements in 3D, particularly with respect to ergonomics. For example, the three parts of the deltoid muscle of the human shoulder are extensively used when pointing in 3D, but each of them has a distinct spatial activation pattern. Figure 2(a) shows that the movements with the highest activation of the anterior deltoid are found in the left half of the movement space, whereas the lateral and posterior deltoids have different patterns in the right and top-right corner.

Figure 2(c) shows how different muscle groups are activated when performing in the upper, middle, and lower parts of the egocentric space. Both examples show that there is a strong connection between the activation of muscles and the spatial location

[2]Marginal improvements to prediction accuracy can be obtained with *Computer Muscle Control*, which is, however, computationally more expensive.

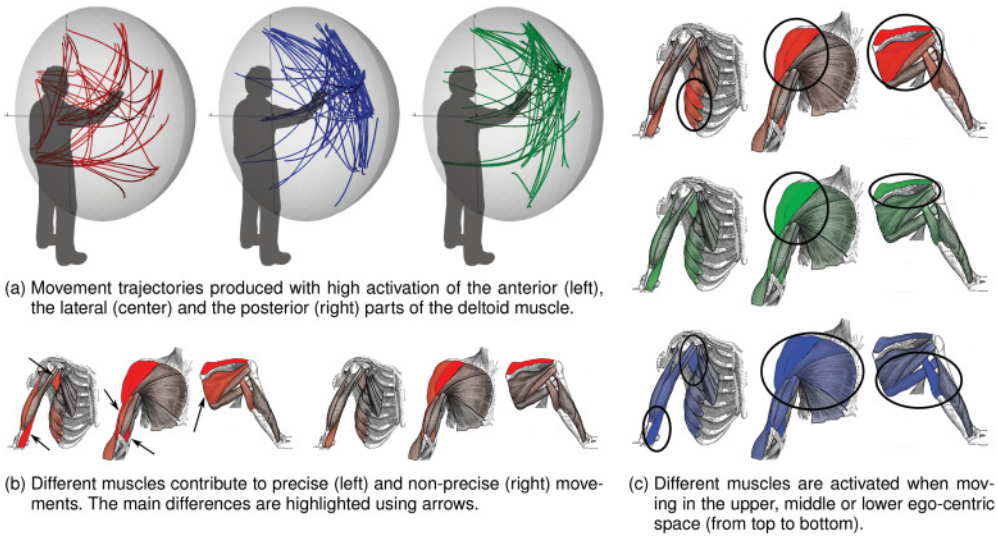


Fig. 2. Overview of the nonuniformity in the dataset. The three plots show how aimed movements in 3D space are non-uniform with respect to the recruitment of muscles for movements with different properties. Color saturation in (b) and (c) indicates the strength of the muscle activation.

of the performance. Figure 2(b) shows that there is also a strong relation between performance and ergonomics. We bisected the dataset into movements with high and low precision by splitting it on mean accuracy, and we visualize the muscle activations for these two sets. It can clearly be seen that specific muscles are more activated in order to produce precise aimed movements. Again, this confirms the nonuniformity of aimed movements in 3D.

## 5. CLUSTERING

The collected dataset represents aimed movements of all lengths, in all directions, and in all locations of the reachable space. In this section, we develop a comprehensive clustering that helps in understanding the ergonomic and performance impacts of design choices. We capture the differences and similarities of muscle activations using the following approach: we cluster all movements based on the temporal muscle activation patterns. Section 5.1 explains this in detail. The result is a comprehensive set of 11 clusters, each with distinctive ergonomic and performance costs of aimed movements in specific regions of the egocentric space (Section 5.2). As we show later in our applications, these clusters are a great resource to include biomechanical information into the design process without running a full-blown study with biomechanical simulation.

### 5.1. Method

Muscle activations are time-dependent functions. Our dataset describes each movement with a family of 41 time-dependent muscle activations: one for each muscle. We call this the *muscle activation pattern* of a movement. Figure 3 shows these patterns for three movements in our dataset. Note how these muscle activations are changing over time: For example, accelerating the arm recruits different muscles than decelerating.

The goal of clustering is to identify movements that are similar to each other with respect to their muscle activation patterns. In the dataset, muscle activations are represented by vectors of varying length, as initially movements have different time lengths and are sampled uniformly at constant intervals. To allow clustering of activations,

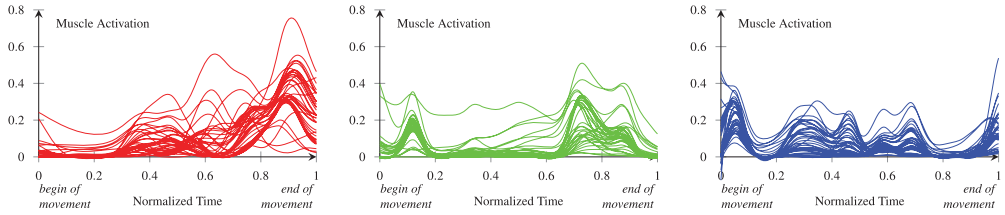


Fig. 3. Muscle activations of three different movements. A movement is characterized by the time-dependent activation of muscles (here: 41). The clustering is based on these muscle activations and assigns similar ones into the same cluster.

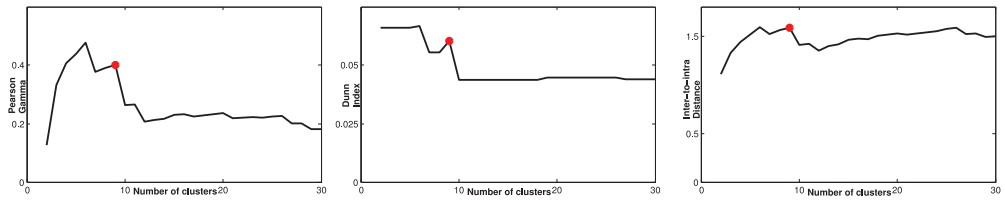


(a) Pearson Gamma (b) Dunn Index (c) Inter-to-intra Ratio

Fig. 4. Quality measures for the clustering aid in selecting an appropriate number of clusters.

we normalize them by time and represent each movement with the same number of samples, namely 40. The samples are computed as mean activations of all muscles within equal-length segments and are concatenated into a single vector; this is a compact representation of the muscular activity for each movement, which is later used for clustering. All other analysis steps are performed on the original muscle activations.

We use an agglomerative hierarchical clustering [Hastie et al. 2009], which provides different levels of abstraction and does not impose assumptions about the distributions. We use Euclidean distance for the clustering because activations at any time or in any muscle have the same effect on the measure. Moreover, absolute values are appreciated, which is important in our setting. In contrast, the Pearson correlation would ignore absolute values. We use Ward's minimum variance linkage method [Ward Jr. 1963], because it creates compact spherical clusters.

In addition, we tried different clustering methods and distance measures (*k-means*, *hierarchical clustering* with *Ward*, *single*, *complete*, *average,* and *centroid* linkage methods, and *Euclidean*, *maximum,* and *Manhattan* distances) and compared their results. The clusters created across all distance measures contain much overlap, but *Manhattan* distance preferred more directionality over co-location in the space, and clusters created with *maximum* distance were less prominent in 3D space than with other distances. We conclude that *Euclidean* distance not only matched our assumptions best, but also performed better than others in the production of interpretable clusters. Among linkage methods, differences were more radical. *Single* and *centroid* linkage methods performed the worst: At each level of hierarchy, they add a single movement to one already existing cluster, and all non-added movements are considered as separate clusters. *Complete* and *average* linkage methods performed slightly better than *single* linkage, but still they kept most movements in a single cluster, and all other clusters contained fewer than 10 movements each. *K-means* for numbers of clusters near 20 produced clusters that strongly overlap with the clusters identified by the hierarchical *Ward* method, but some of them simultaneously span similar locations in 3D space. For smaller numbers of clusters, *k-means* produced clusters that are hard to interpret. Among methods we tried, hierarchical clustering with the *Ward* linkage

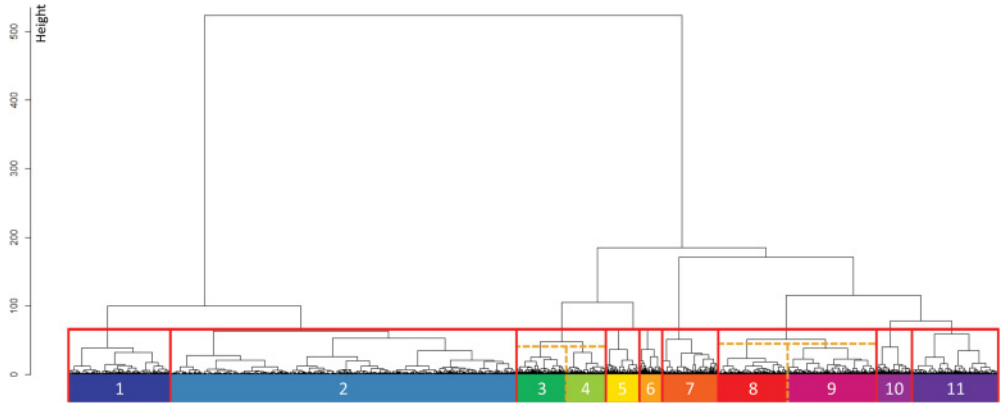


Fig. 5. Dendrogram showing the hierarchical structure of the whole dataset. Red lines cut the dataset into clusters at the height selected by the goodness-of-clustering criteria, orange dashed lines correspond to the cuts performed manually.

method and *Euclidean* distance produced clusters that were most interpretable with respect to 3D location and direction and of acceptable size.

For the clustering method we chose, Figure 5 shows the hierarchy of the resulting clusters in the form of a dendrogram. As can be seen, we selected different levels in the hierarchy for different clusters. This was done in a semiautomatic fashion informed by three quality measures for hierarchical clustering: Figure 4 shows the *Pearson gamma*, the *Dunn index*, and the *inter-to-intra* cluster ratio. We have also checked other cluster quality indices such as *average silhouette width*, *Calinski* and *Harabasz index*, *Goodman* and *Kruskal's Gamma coefficient*, and *G3 coefficient,* and they show similar patterns of *bumps* or *elbows* on the plot for the particular cluster number. These quality measures show that six and nine clusters are good choices. When choosing six clusters, distinctions between clusters in 3D location and movement directionality are weaker or even degraded; for example, Cluster 5 and Cluster 6 are combined into a single cluster although they correspond to movements on opposite parts of space. When choosing more clusters, they become more compact in 3D space and exhibit even more similarity in movement direction, but, as a downside, multiple clusters start to span the same space, which also affects interpretability. We decided in favor of nine clusters because they were more interpretable for humans—this is important, since this clustering is supposed to be read and understood by humans when designing interfaces, rather than by a machine. Finally, we inspected these clusters and split two clusters one more time (by choosing the next level in the hierarchy for them) in order to obtain an even more human-interpretable result, as can be observed in Figure 7. The final number of clusters is 11. We have also analyzed the dendrogram at each split to extract any semantic interpretation of why the split occurred. We considered the most prominent differences between mean values of two clusters under the split as a semantic description of the split (Figure 6), although small differences were present in the patterns of most muscles.

### 5.2. Overview of Clustering

Figure 8 shows details about the movements in each cluster: their performance, their ergonomics, and their location in 3D, as well as the main directions of the movements. In particular, we show:

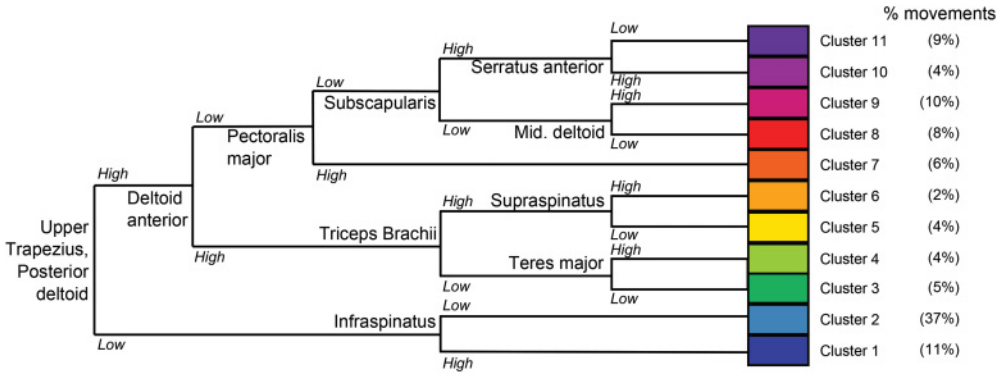


Fig. 6. Semantic representation of the dendrogram. The splits in this hierarchy are named after the muscle with the highest activation difference between the split sets. See text for details about choosing the levels.

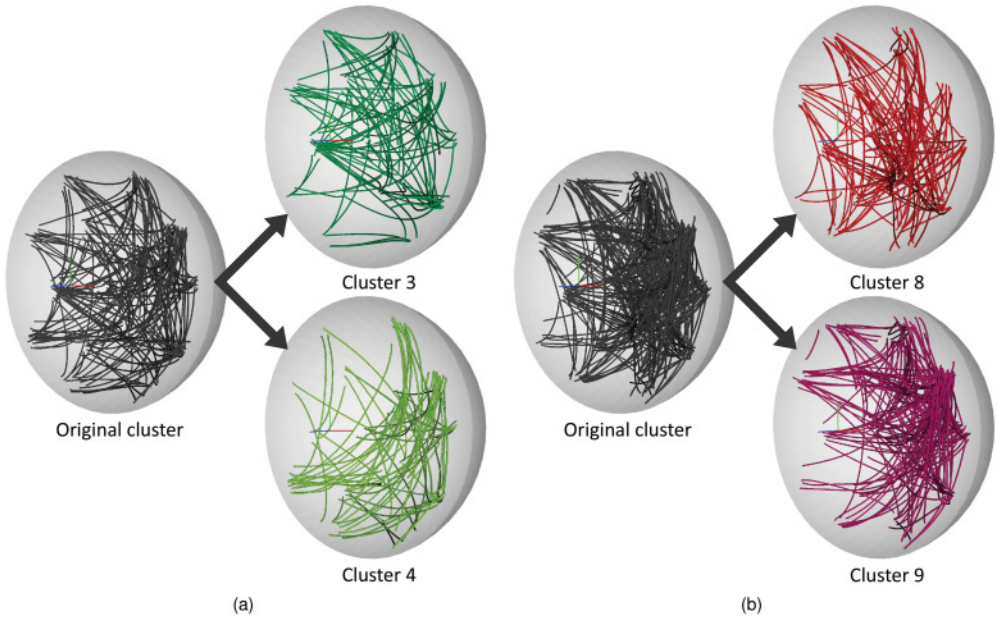


Fig. 7. The clusters are manually split on the next level of the dendrogram to become better interpretable in 3D space and movement directionality. As can be observed here, it is hard to identify any pattern in the original clusters, but, after the splits, it is clearly visible that Cluster 3 contains long and middle-length movements in the central and upper part of the space, directed diagonally closer to horizontal; Cluster 4 contains long, close to vertical movements in the right upper part of the space, smoothly transitioning through close to diagonal movements in the lower right part of the space, to close to horizontal movements in the lower left part of the space; Cluster 8 contains long movements between opposite parts of the space; and Cluster 9 contains medium and long slightly diagonal and close to horizontal movements mostly in the right and central parts of the space.

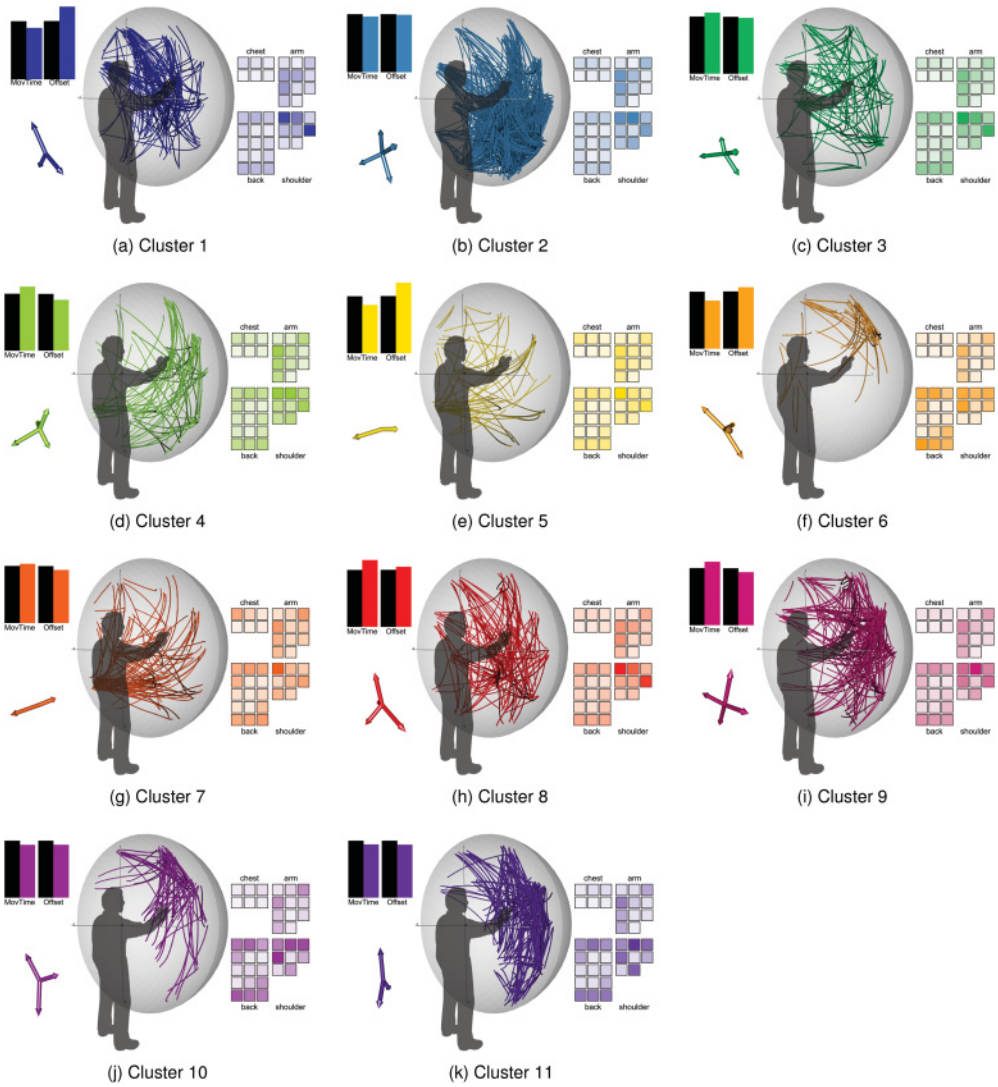


Fig. 8. Each subfigure shows performance (barplots), ergonomics (LED visualization), and spatial information (3D trajectories and oriented arrows) for the final 11 clusters. The opacity of each LED is defined according to the average activation of the corresponding muscle in the current cluster. See Figure 9 for the legend.

—**performance:** two groups of bar plots representing the average movement time and offset. We used black for the overall value and colors for the values of the respective clusters;
—**ergonomics:** activation of the four main areas of the upper part of the human body: shoulder, chest, back, and arm;
—**spatial information:** 3D trajectories of the involved movements and arrows oriented according to their main directions.

This overview shows, on the one hand, the nonuniformity of the movement space, yet, on the other hand, each cluster contains movements that share similarities regarding

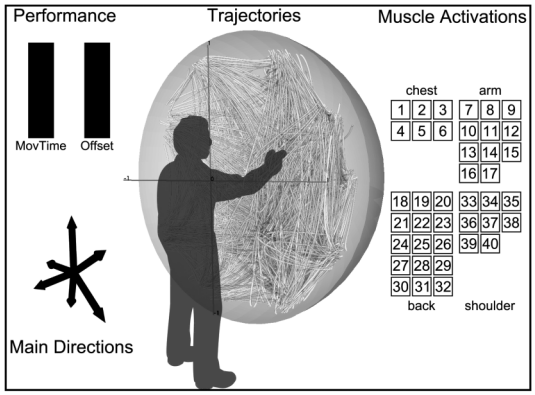


Fig. 9. Legend for the cluster representation in Figure 8. The muscles represented in the LED visualization are: 1–3 Pectoralis major, 4–6 Pectoralis minor, 7 Coracobrachialis, 8 Supinator brevis, 9 Triceps longhead, 10 Brachialis, 11 Biceps longhead, 12 Triceps lateralis, 13 Pronator teres, 14 Biceps shorthead, 15 Triceps medialis, 16 Brachioradialis, 17 Anconeus, 18–21 Trapezius, 22–23 Rhomboid major, 24–26 Latissimus dorsi, 27–32 Serratus anterior, 33–35 Deltoid, 36 Supraspinatus, 37 Teres minor, 38 Infraspinatus, 39 Teres major, 40 Subscapularis.

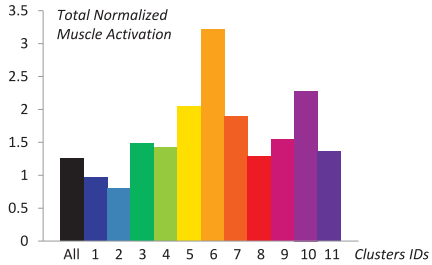


Fig. 10. Total normalized muscle activations for each cluster.

its spatial information and other attributes. This is important for their interpretation and their later use for guiding User Interface (UI) design.

This clustering confirms our results from the previous section. For example, we looked at the spatial distribution of the movements for the three deltoid muscles on the shoulder (Figure 2(a)). These movements are contained in Clusters 6, 10, 11 and 7, which have a high shoulder activation. Furthermore, we examined the muscle activations for precise and nonprecise movements (Figure 2(b)). We saw that, in general, the chest and shoulder muscles are more activated in the case of precise movements. This trend is also shown in Figure 8, where clusters with the highest precision (Clusters 4, 9, 10, and 11) present a high activation in the same areas.

The total normalized muscle activations for each cluster are reported in Figure 10. Note the clear differences between the clusters, which serves as another indicator for a good clustering.

### 5.3. Description of Clusters

We make the following observations about each cluster:

**Cluster 1** covers short and middle-length movements in the central and left upper parts of the space, directed diagonally closer to vertical. This cluster exhibits lower than average throughput of movements; in particular, a small advantage in speed is counterbalanced with a two times greater drawback in accuracy. Muscle activations are

high for the infraspinatus and anterior deltoid; medium for medial deltoid, brachialis, and biceps; and low for all other muscles. Movements in this cluster are suitable for short-term interaction, for alternation with other clusters, or in exergaming to train the anterior deltoid.

**Cluster 2** covers short and middle-length movements in the lower right and central parts of the space in all directions and some long vertical movements in the middle part of the space. This cluster has slightly higher than average throughput of movements; improvements are present in both accuracy and speed. Muscle activations are high only for the medial deltoid; medium for anterior deltoid, brachialis, pronator teres and infraspinatus; and low for all other muscles. This cluster exhibits better than average performance and optimal energy expenditure, which makes it suitable for the majority of interfaces that need long-term interaction. Exergames within this cluster would not be effective.

**Cluster 3** covers long and middle-length movements in the central and upper part of the space, directed diagonally closer to horizontal. This cluster exhibits lower than average throughput of movements; in particular, a slight advantage in accuracy is counterbalanced by a twice greater drawback in speed. Muscle activations are high for the infraspinatus and anterior deltoid; medium for medial deltoid, supraspinatus, serratus anterior, brachialis, pronator teres, upper trapezius, and romboid major; and low for all other muscles. Movements within this cluster can be used for short-term interaction with huge public displays, where large movements are necessary, or for sports exergames (e.g., tennis).

**Cluster 4** covers long, close to vertical movements in the right upper part of the space, smoothly transitioning through close to diagonal movements in the lower right part of the space, to close to horizontal movements in the lower left part of the space. This cluster has slightly lower than average throughput; in particular, an increase in accuracy is strongly counterbalanced by a decrease in speed. Muscle activations are high for the anterior and medial deltoids, infraspinatus, and brachialis; medium for posterior deltoid, supraspinatus, triceps, pronator teres, and part of the trapezius; and low for all other muscles. Movements within this cluster are close to the movements performed in sports, as in tennis or golf. It can be used for exergames and for training.

**Cluster 5** covers short and middle-length horizontal movements in the left and central part of the space. This cluster has lower than average performance; the accuracy is 1.5 times lower than the speed is higher. Muscle activations are high for the anterior deltoid and infraspinatus; medium for brachialis, pronator teres, and trapezius; and low for all other muscles. Movements in this cluster are suitable for low-accuracy interaction, for exergames, or primitive interactions with smartwatches.

**Cluster 6** covers short and medium diagonal close to horizontal movements in the topmost part of the space. The performance is slightly higher than average; a small decrease in accuracy is compensated for by a twofold increase in speed. Muscle activations are high for all deltoids, supraspinatus, brachialis, trapezius, and serratus anterior; medium for triceps, pronator teres, brachioradialis, romboid major, and infraspinatus; low for the rest of the muscles. Movements within this cluster can be used for training of multiple shoulder muscles.

**Cluster 7** covers medium-length and long movements between the leftmost lowest point and other parts of the space. This cluster has slightly higher than average performance, with better accuracy and lower speed. Muscle activations are high for the anterior deltoid; medium for other deltoids, teres minor, triceps, brachialis, brachioradialis, pronator teres, pectoralis major, serratus anterior, trapezius, rhomboid, infraspinatus, and teres major; low for a few other muscles. Movements within this cluster are the least convenient compared to other clusters, and their usage should be avoided.

**Cluster 8** covers long movements between opposite parts of the space. This cluster has 20% lower performance, resulting in both lower accuracy and much lower speed. Muscle activations are high for anterior deltoid and infraspinatus; medium for brachialis and pronator teres; and low for all other muscles. Movements within this cluster can be used for short interaction, alternation between types of load, or for exergames.

**Cluster 9** covers medium and long diagonal and close to horizontal movements mostly in the right and central parts of the space. This cluster has lower than average performance; in particular, accuracy is slightly higher and speed is almost twice as low. Muscle activations are high for the medial deltoid; medium for other deltoids, supraspinatus, infraspinatus, and brachialis; and low for all other muscles. Movements within this cluster are suitable for short-term interaction or for alternation between loaded muscles.

**Cluster 10** covers short and medium movements in the upper right part of the space in diagonal and mostly very close to vertical directions. This cluster has higher than average performance; both accuracy and speed are approximately 6% higher. Muscle activations are high for the posterior and medial deltoids, infraspinatus, upper trapezius, and serratus anterior; medium for anterior deltoid; and low for all other muscles. This cluster can be used for short-term interaction, for alternation, and for interactions where high throughput is necessary.

**Cluster 11** covers short and medium mostly vertical movements in the right part of the space. This cluster exhibits higher than average performance; both accuracy and speed are 6% higher. Muscle activations are high for the medial deltoid, supraspinatus, upper trapezius, and subscapularis; medium for serratus anterior, anterior and posterior deltoids, and brachialis; and low for all other muscles. This cluster can be used for medium-term interaction or for alternation between muscle loads.

### 5.4. Performance Analysis

We computed Fitts's law models [MacKenzie 1992] for each cluster separately and compared fitness for a model computed for the whole dataset. We used the standard model introduced earlier, with $a$ and $b$ fit to subsets of movements defined by the clusters. As Figure 11 shows, the model fit per cluster is higher than for the whole dataset. The average model fit per cluster was $R^2 = .97$, whereas the fit for the whole dataset was $R^2 = .95$. This corroborates the plausibility of the clustering. The models show up to 28% difference in throughput between the clusters. Details of performance analysis of each particular cluster are given in Figure 11, as well as in the context of each cluster in Section 5.3.

## 6. APPLICATIONS

The typical approach to assessing the efficiency of input methods employs empirical studies. The proposed clustering allows any given *input region* to be examined for muscle load and user performance prior to such studies, or even instead of such studies. The clustering can be applied in many scenarios by following this scheme:

(1) Identify characteristic properties of the involved movements: their length, their directions, and the 3D volume in which the movements are to be sensed.
(2) Use Figure 8 and the corresponding descriptions from Section 5 to identify the clusters that strongly intersect that input volume.
(3) Among these candidate clusters, find those that contain movements with the desired length and directions.
(4) Finally, examine the performance and ergonomic properties of these clusters and choose the one that is most suitable for the application.

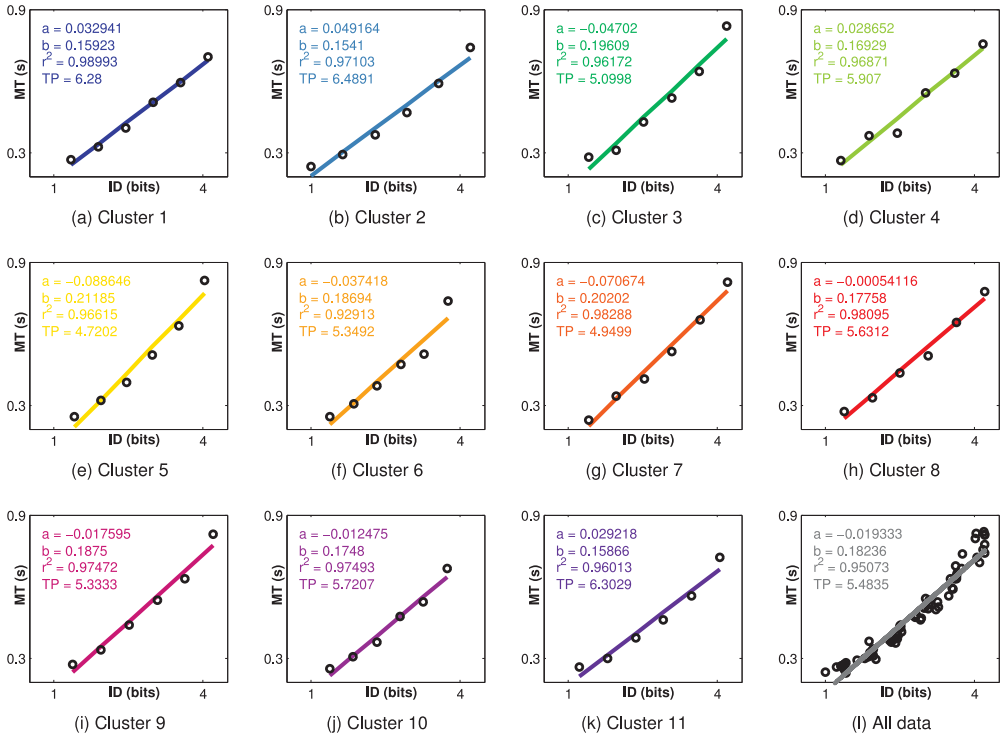


Fig. 11. Fitts's law models for the clusters show that improvements to fitness can be obtained by knowing the clusters.

To illustrate some applications and evaluate our clustering, we consider four cases of UI design: (1) in-air keyboard placement, (2) public display interaction, (3) tabletop interaction, and (4) in-air input for a smartwatch.

As argued earlier, the clusters represent an upper bound on performance. The properties of the particular input method and the skills of the user are further aspects of the performance.

### 6.1. Case 1: In-Air Keyboard Placement

Here, we describe an exercise to inform the design of virtual keyboards operated by gesturing or pointing with the arm in mid-air [Ni et al. 2011; Shoemaker et al. 2009; Jones et al. 2010]. Such a keyboard can be implemented with multiple sensors (e.g., accelerometers and computer vision) and interaction techniques (e.g., selection- or gesture-based) and are already used in console games (e.g., for the Nintendo Wii and in Microsoft Kinect). One outstanding question is the placement of the *input region*: how to position the movements required for typing in the space within reach of a user's arm. Previous empirical studies have compared in-air keyboards of different sizes and at different distances [Shoemaker et al. 2009; Jones et al. 2010]. These parameters affect the angle and extension of the arm in the reachable space. An ideal area would allow the maximum number of words per minute (wpm) to be typed with a low level of muscle fatigue that warrants sustained typing.

We now examine our clustering. We have two main physical constraints:

—the cluster needs to cover a space large enough for a keyboard,
—and the movements in this cluster need to be short enough to support typing on reasonably sized virtual keys.

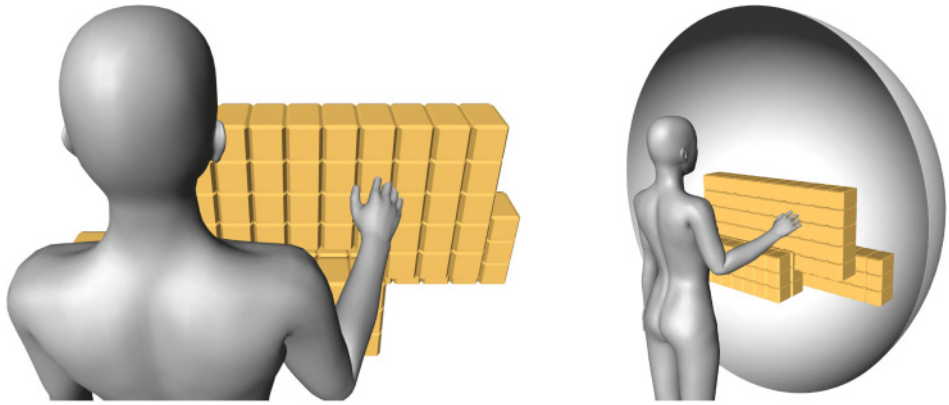

Fig. 12. The optimal input region for a virtual keyboard lies within Cluster 2 (see also Figure 8). This cluster has a good accuracy for aiming movements in a space that is large enough to host a virtual keyboard. Furthermore, the ergonomics in this cluster are very good: It has the lowest total normalized muscle activation (see also Figure 10).

Four clusters fulfill these constraints: 1, 2, 9, and 11. As we know from Figure 8, the offset (inaccuracy) in Cluster 1 is rather high, so we exclude it. Among the remaining clusters, Cluster 2 has the lowest total normalized muscle activation (Figure 10). Hence, this cluster is a good place for the keyboard.

To evaluate this finding, we employ the following computational approach on the original (unclustered) dataset: The goal is to find input regions for a keyboard with the best pointing performance and a low level of muscle activation. As the performance measure, we use throughput calculated from the *effective* index of difficulty: $TP = ID_e/MT$. For the ergonomics index, we use *total muscle activation integrated over time per unit length*, which allows the comparison of movements with different amplitude.

We chose a $10 \times 3$ button arrangement for the keyboard, which allows us to implement a Qwerty layout. The choice of a button size of 7cm is based on the distribution of the pointing inaccuracy observed in the data. This leads to an overall keyboard size of $70\text{cm} \times 21\text{cm}$ for width and height, respectively. We computationally move this keyboard design in the reachable space to find its best placement. To do so, we divide the 3D space into a regular grid of equidistant points and calculate the average throughput for movements within the associated volumes.

The best volumes for placement of such a keyboard are shown in Figure 12. We observe that the best placements are generally in the central-lower part of the egocentric space. Two alternatives are provided: The dominant arm is extended and operates on either the contralateral (left) or lateral (right) side.

Most importantly, the computational placement coincides with Cluster 2. This confirms the utility of the clustering.

### 6.2. Case 2: Public Display

If designing user interfaces was simply about their ergonomics, then we would just select the regions where movements require a low average muscle activation. However, designing good user interfaces is not that simple. Many constraints need to be met: Movements may be restricted to a certain region, direction, and/or length, and so on.

Take a public display, for example, as shown in Figure 13: It is mounted to the wall at a certain height, and the user has to maintain a certain distance from the display to read it properly. Furthermore, the movements are only two-dimensional on the surface of the display. These constraints are shown in Figure 13(b).

(a) Real-life example of a public display.

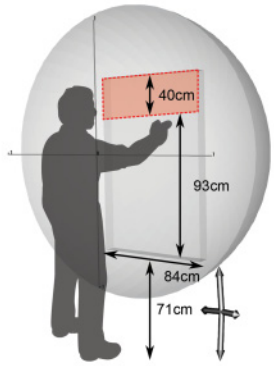


(b) Conceptual image showing size and position of the device in 3D space together with the main directions of the involved movements.

**% Movements:**
Cluster 1: 23%
Cluster 2: 9%
Cluster 3: 8%
Cluster 9: 53%
Cluster 11: 7%
**Statistical results:**
Offset to target center: 48 mm
Movement time: 449 ms
Throughput: 5.52 bits/s
Total normalized
muscle activation: 1.5

(c) Results: percentage of the involved movements for each cluster and additional statistical data.

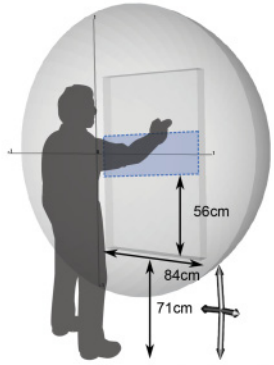


(d) Conceptual image showing a lowered interaction area.

**% Movements:**
Cluster 2: 100%
**Statistical results:**
Offset to target center: 44 mm
Movement time: 204.8 ms
Throughput: 5.57 bits/s
Total normalized
muscle activation: 0.55

(e) Results: percentage of the involved movements for each cluster and additional statistical data for the lowered interaction area.

Fig. 13. We examined muscle load and user performance for the region on a vertical public display containing an interactive menu. Starting from a real life example *(a)*, we extracted its spatial setup and the main directions of its movements *(b)*. Using Figure 8, we identified the clusters that contain the desired movements: 1 and 9. Because these two clusters are not suitable for long-term interactions, we lowered the region to bring all movements to Cluster 2 *(d)*. As a result, the movements have better performance and lower ergonomic costs. More accurate cluster intersecting percentages and average performance and ergonomics values are shown in *(c)* and *(e)*.

In our example, a region containing an interactive menu is placed in the upper part of the device, as shown in Figure 13(b). As we can see from Figure 8, the interaction with this display falls mostly into Clusters 1 and 9. This is also confirmed by a computational analysis using the original dataset: The precise percentages of the intersection and additional information about the user's performance and muscle load are given in Figure 13(c). Such computational analysis was performed by specifying a 3D representation of the interaction area and immersing it in the virtual space of the recorded trajectories.

As we know from our cluster analysis in Section 5.3, Clusters 1 and 9 are good for short-term interactions, but they should not be used for long-term, sustained interactions. Hence, this may not be the best location for a menu with involved interactions since users will fatigue too quickly.

(a) Real-life example of a tabletop.

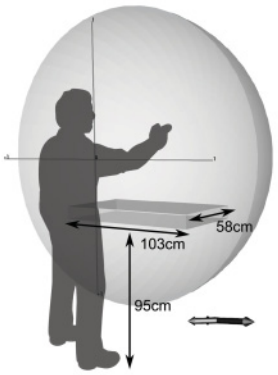


(b) Concept image of the tabletop case showing its spatial setup and the main directions of the involved movements.

**% Movements:**

Cluster 2: 74%
Cluster 3: 5%
Cluster 4: 12%
Cluster 5: 4%
Cluster 9: 4%
Cluster 11: 1%

**Statistical results:**

Offset to target center: 33.6 mm
Movement time: 442.2 ms
Throughput: 6.2 bits/s
Total normalized
muscle activation: 1.06

(c) Results: percentage of the involved movements for each cluster and additional statistical data.

Fig. 14. We examined user's performance and muscle load for a tabletop. Taking a real example of the device *(a)*, we defined the setup of its volume, its position in space. and the main directions of its movements *(b)*. By examining Figure 8, we identified the involved clusters: 2 and 4. More accurate cluster intersecting percentages and average performance and ergonomic values are shown in *(c)*.

To address this issue, we lowered the position of the interaction area to make it intersect Cluster 2. From Section 5.3, we know that this cluster is suitable for long-term interactions. The resulting area is represented in *blue* in Figure 13(d). Figure 13(e) shows clearly both the improvement of the user's performance and the decrease of the ergonomic costs.

### 6.3. Case 3: Tabletop

In Figure 14. we analyzed an interaction scenario with a horizontal tabletop. In this setup, the involved movements are mostly horizontal and from front to back. Figure 8 informs us that the involved movements are mostly contained in Clusters 2 and 4. More precise percentages of the intersection and additional information about the user's performance and muscle load are given in Figure 14(c).

This scenario is significantly better suited for text entry than the public display from the previous case: Movements in Cluster 2 are accurate and have a low muscle activation.

### 6.4. Case 4: Smartwatch Input

Our fourth case concerns the design of input for smartwatches [Narayanaswami and Raghunath 2000]. The largest drawback of these devices is the very limited input space due to the small form-factor. The number of buttons on such a device is very small. Multitouch interfaces are not suitable due to the tiny screen and the occlusions that would be caused by the hand. One of the alternatives for increasing the input space is to capture mid-air gestures using an integrated camera.

We analyze here two options of camera placement for gestural interaction: The first option (Figure 15(a)) is used in the recently released *Samsung Gear*. The second option (Figure 15(d)) is our alternative to it, informed by our dataset and clustering.

The camera placement in Figure 15(a) requires the user to enter gestures with the right arm in the left contralateral part, namely in Clusters 1 and 9. Our alternative design, on the other hand, features a camera facing to the right of the smartwatch, as demonstrated in Figure 15(d). This would allow interaction in Cluster 2, which is two times less fatiguing and provides higher accuracy and performance.

(a) Real-life example of a smartwatch. Interaction volume for the camera placement of Samsung Gear.

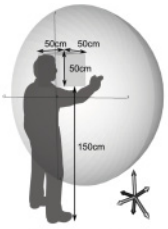


(b) Conceptual image showing size and position of the interaction volume in 3D space together with the main directions of the involved movements.

**% Movements:**

Cluster 1: 65%
Cluster 9: 35%

**Statistical results:**

Offset to target center: 59.8 mm
Movement time: 404 ms
Throughput: 4.7 bits/s
Total normalized
muscle activation: 1.7

(c) Results: percentage of the involved movements for each cluster and additional statistical data.

(d) Real-life example of a smartwatch. Interaction volume for an alternative camera placement.

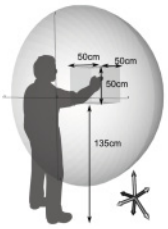


(e) Conceptual image showing size and position of the interaction volume in 3D space together with the main directions of the involved movements.

**% Movements:**

Cluster 2: 100%

**Statistical results:**

Offset to target center: 60.8 mm
Movement time: 442.5 ms
Throughput: 5.9 bits/s
Total normalized
muscle activation: 0.8

(f) Results: percentage of the involved movements for each cluster and additional statistical data.

Fig. 15. We examined the muscle load and user performance for gestural input to a smartwatch. We considered two alternative interaction volumes depending on camera placement and direction (upper, Samsung Gear case; lower, alternative case). Starting from real-life examples *(a, d)*, we extracted the spatial setup of the corresponding interaction volumes and the main directions of their movements *(b, e)*. Using Figure 8, we identified the clusters that contain the desired movements: Clusters 1 and 9 for the first case, and Cluster 2 for the alternative case. More accurate cluster intersecting percentages and average performance and ergonomic values are shown in *(c, f)*.

## 7. SUMMARY AND DISCUSSION

The long-term goal of our work is to facilitate the use of biomechanical simulation data in user interface design. Biomechanical simulation yields a rich description of observed movement, including time-dependent angles, forces, and torques at joints, as well as activations and loads for muscles. Combined with performance modeling, it could play a major role in the design of novel UIs. Indeed, although the ergonomics of desktop-based interfaces have been heavily studied, interactions "beyond the desktop" clearly need more attention.

The approach presented here could accelerate design by allowing first estimates without expensive empirical investigations. It bypasses the numerous steps of the standard pipeline of motion capture-based biomechanical simulation. The clusters can inform UI design in two ways: First, given movement parameters (location, direction, amplitude) assumed by a design, the clusters can estimate the muscle loads and user performance (speed, accuracy, throughput). Second, given target values for muscle loads or performance, the clusters will give information on which location, direction, and amplitude are feasible as input. We have shown four examples for interface design.

The clustering was made possible by extending the *data-driven approach* [Flanders 1991; Micera et al. 1999, 2000] to biomechanical simulation of pointing movements covering the whole reachable space of the arm and associated with performance metrics. The resulting clustering is a summarization of the main muscle activation patterns that describe pointing tasks with the arm. It is striking that the very complex coordinated action of tens of muscles and joints can be described in as few as 11 clusters. The clusters

capture some major effects of nonuniformity and expose significant differences among seemingly similar movements.

Although the results are already applicable for in-air interfaces, the approach permits extensions to other UIs. We are working on two technical issues that need to be resolved to expand applicability: (1) dynamic contact forces in touch-based interactions and (2) simulation of the fine motor movements of fingers [Bachynskyi et al. 2014]. For example, in our application Cases 2 and 3, our cluster-based analysis did not take into account the effect of friction (finger pulp contacting the surface). In principle, the approach will be suitable for design problems that involve (1) aimed movements, (2) a large movement space, and (3) a nontrivial ergonomics issue. For example, a recent paper on multitouch rotations concluded that rotations on a tabletop are biomechanically very heterogeneous, and more research is needed to find a link to performance and physical ergonomics [Hoggan et al. 2013]. Another recent example is interaction with a thumb on a touchscreen display [Trudeau et al. 2012a, 2012b]. The present approach could be used to segment the input space according to performance and the amount of extension/flexion required.

To allow other groups to benefit from the large amount of valuable data gathered in this work, we release our data to the community under the following link: http://resources.mpi-inf.mpg.de/coactivationclustering.

## REFERENCES


Sergei Adamovich, Michail Berkinblit, Olga Fookson, and Howard Poizner. 1999. Pointing in 3D space to remembered targets II: Effects of movement speed toward kinesthetically defined targets. *Experimental Brain Research* 125, 2 (1999), 200–210.

Myroslav Bachynskyi, Antti Oulasvirta, Gregorio Palmas, and Tino Weinkauf. 2013. Biomechanical simulation in the analysis of aimed movements. In *CHI'13 Extended Abstracts on Human Factors in Computing Systems (CHI EA'13)*. ACM, New York, NY, 277–282. DOI:http://dx.doi.org/10.1145/2468356.2468406

Myroslav Bachynskyi, Antti Oulasvirta, Gregorio Palmas, and Tino Weinkauf. 2014. Is motion capture-based biomechanical simulation valid for HCI studies?: Study and implications. In *Proceedings of the 32nd Annual ACM Conference on Human Factors in Computing Systems (CHI'14)*. ACM, New York, NY, 3215–3224. DOI:http://dx.doi.org/10.1145/2556288.2557027

Amartya Banerjee. 2012. *Remote Multitouch: In-air Pointing Techniques for Large Display Interactions*. Master's thesis. Queen's University, Kingston, Ontario, Canada.

Gabriel Baud-Bovy and Paolo Viviani. 1998. Pointing to kinesthetic targets in space. *The Journal of Neuroscience* 18, 4 (1998), 1528–1545.

Roberto Caminiti, Paul B. Johnson, Cesare Galli, Stefano Ferraina, and Yves Burnod. 1991. Making arm movements within different parts of space: The premotor and motor cortical representation of a coordinate system for reaching to visual targets. *The Journal of Neuroscience* 11, 5 (1991), 1182–1197.

Roberto Caminiti, Paul B. Johnson, and Antonio Urbano. 1990. Making arm movements within different parts of space: Dynamic aspects in the primate motor cortex. *The Journal of Neuroscience* 10, 7 (1990), 2039–2058.

Yeonjoo Cha and Rohae Myung. 2013. Extended Fitts' law for 3D pointing tasks using 3D target arrangements. *International Journal of Industrial Ergonomics* 43, 4 (2013), 350–355.

Ankit Chaudhary, Jagdish Lal Raheja, Karen Das, and Sonia Raheja. 2013. Intelligent approaches to interact with machines using hand gesture recognition in natural way: A survey. *arXiv preprint arXiv:1303.2292* (2013).

David J. Cooke and Susan H. Brown. 1994. Movement-related phasic muscle activation. *Experimental Brain Research* 99, 3 (1994), 473–482.

Paolo de Leva. 1996. Adjustments to Zatsiorsky-Seluyanov's segment inertia parameters. *Journal of Biomechanics* 29, 9 (1996), 1223–1230. DOI:http://dx.doi.org/10.1016/0021-9290(95)00178-6

Scott L. Delp, Frank C. Anderson, Allison S. Arnold, Peter Loan, Ayman Habib, and others. 2007. Opensim: Open-source software to create and analyze dynamic simulations of movement. *IEEE Trans. Biomedical Engineering* 54, 11 (2007), 1940–1950. http://citeseerx.ist.psu.edu/viewdoc/summary?doi=10.1.1.95.5297

Scott L. Delp, Srikanth Suranarayanan, Wendy M. Murray, Jim Uhlir, and Ronald J. Triolo. 2001. Architecture of three major trunk muscles. *Journal of Biomechanics* 34 (2001), 371–371.

Paul M. Fitts. 1954. The information capacity of the human motor system in controlling the amplitude of movement. *Journal of Experimental Psychology* 47, 6 (1954), 381.

Martha Flanders. 1991. Temporal patterns of muscle activation for arm movements in three-dimensional space. *The Journal of Neuroscience* 11, 9 (1991), 2680–2693.

Hans-Joachim Freund and Hans-Joachim Büdingen. 1978. The relationship between speed and amplitude of the fastest voluntary contractions of human arm muscles. *Experimental Brain Research* 31, 1 (1978), 1–12.

Luigi Gallo, Alessio Pierluigi Placitelli, and Mario Ciampi. 2011. Controller-free exploration of medical image data: Experiencing the kinect. In *Proceedings of the 2011 24th International Symposium on Computer-Based Medical Systems (CBMS'11)*. IEEE, 1–6. DOI:http://dx.doi.org/10.1109/CBMS.2011.5999138

Stan C. A. M. Gielen, K. Van den Oosten, and F. Pull ter Gunne. 1985. Relation between EMG activation patterns and kinematic properties of aimed arm movements. *Journal of Motor Behavior* 17, 4 (1985), 421–442.

Paul L. Gribble, Lucy I. Mullin, Nicholas Cothros, and Andrew Mattar. 2003. Role of cocontraction in arm movement accuracy. *Journal of Neurophysiology* 89, 5 (2003), 2396–2405.

Tovi Grossman and Ravin Balakrishnan. 2004. Pointing at trivariate targets in 3D environments. In *Proceedings of the SIGCHI Conference on Human Factors in Computing Systems*. ACM, 447–454.

Christopher M. Harris and Daniel M. Wolpert. 1998. Signal-dependent noise determines motor planning. *Nature* 394, 6695 (1998), 780–784.

Trevor Hastie, Robert Tibshirani, and Jerome Friedman. 2009. *The Elements of Statistical Learning: Data Mining, Inference, and Prediction* (2nd ed.). Springer.

Errol R. Hoffmann, Colin G. Drury, and Carol J. Romanowski. 2011. Performance in one-, two- and three-dimensional terminal aiming tasks. *Ergonomics* 54, 12 (2011), 1175–1185.

Eve Hoggan, John Williamson, Antti Oulasvirta, Miguel Nacenta, Per Ola Kristensson, and Anu Lehtiö. 2013. Multi-touch rotation gestures: Performance and ergonomics. In *Proceedings of the SIGCHI Conference on Human Factors in Computing Systems*. ACM, 3047–3050.

Katherine R. S. Holzbaur, Wendy M. Murray, and Scott L. Delp. 2005. A model of the upper extremity for simulating musculoskeletal surgery and analyzing neuromuscular control. *Annals of Biomedical Engineering* 33, 6 (2005), 829–840. http://dx.doi.org/10.1007/s10439-005-3320-7

Di-An Hong, Daniel M. Corcos, and Gerald L. Gottlieb. 1994. Task dependent patterns of muscle activation at the shoulder and elbow for unconstrained arm movements. *Journal of Neurophysiology* 71, 3 (1994), 1261–1265.

Anil K. Jain, M. Narasimha Murty, and Patrick J. Flynn. 1999. Data clustering: A review. *ACM Computing Surveys (CSUR)* 31, 3 (1999), 264–323.

Eleanor Jones, Jason Alexander, Andreas Andreou, Pourang Irani, and Sriram Subramanian. 2010. Gestext: Accelerometer-based gestural text-entry systems. In *Proceedings of the 28th International Conference on Human Factors in Computing Systems*. ACM, 2173–2182.

Andreas Kontaxis, Andrea Giovanni Cutti, Garth R. Johnson, and Dirk-Jan E. J. Veeger. 2009. A framework for the definition of standardized protocols for measuring upper-extremity kinematics. *Clinical Biomechanics* 24 (2009), 246–253.

Gail F. Koshland and Ziaul Hasan. 1994. Selection of muscles for initiation of planar, three-joint arm movements with different final orientations of the hand. *Experimental Brain Research* 98, 1 (1994), 157–162.

Francesco Lacquaniti, John F. Soechting, and S. A. Terzuolo. 1986. Path constraints on point-to-point arm movements in three-dimensional space. *Neuroscience* 17, 2 (1986), 313–324.

Belinda Lange, Chien-Yen Chang, Evan Suma, Bradley Newman, Albert Skip Rizzo, and Mark Bolas. 2011. Development and evaluation of low cost game-based balance rehabilitation tool using the Microsoft Kinect sensor. In *Proceedings of the 2011 Annual International Conference of the IEEE on Engineering in Medicine and Biology Society (EMBC'11)*. IEEE, 1831–1834.

Jui-Feng Lin and Yi-Cheng Ho. 2011. Verification of ballistic movement models in a true 3D environment. In *Proceedings of the 2nd East Asian Ergonomics Federation Symposium*. CRC Press.

Morten Enemark Lund, Mark de Zee, Michael Skipper Andersen, and John Rasmussen. 2012. On validation of multibody musculoskeletal models. *Proceedings of the Institution of Mechanical Engineers, Part H: Journal of Engineering in Medicine* 226 (2012), 82–94.

Scott I. MacKenzie. 1992. Fitts' law as a research and design tool in human-computer interaction. *Human-Computer Interaction* 7, 1 (1992), 91–139.

Scott I. MacKenzie and William Buxton. 1992. Extending Fitts' law to two-dimensional tasks. In *Proceedings of the SIGCHI Conference on Human Factors in Computing Systems*. ACM, 219–226.

Silvestro Micera, Angelo M. Sabatini, and Paolo Dario. 2000. On automatic identification of upper-limb movements using small-sized training sets of EMG signals. *Medical Engineering & Physics* 22, 8 (2000), 527–533.

Silvestro Micera, Angelo M. Sabatini, Paolo Dario, and Bruno Rossi. 1999. A hybrid approach to EMG pattern analysis for classification of arm movements using statistical and fuzzy techniques. *Medical Engineering & Physics* 21, 5 (1999), 303–311.

Akihiko Murai, Kosuke Kurosaki, Katsu Yamane, and Yoshihiko Nakamura. 2010. Musculoskeletal-see-through mirror: Computational modeling and algorithm for whole-body muscle activity visualization in real time. *Progress in Biophysics and Molecular Biology* 103, 2–3 (2010), 310–317. DOI:http://dx.doi.org/10.1016/j.pbiomolbio.2010.09.006 Special Issue on Biomechanical Modelling of Soft Tissue Motion.

Chandrasekhar Narayanaswami and Mandayam T. Raghunath. 2000. Application design for a smart watch with a high resolution display. In *Proceedings of the 4th International Symposium on Wearable Computers*. IEEE, 7–14.

Tao Ni, Doug Bowman, and Chris North. 2011. Airstroke: Bringing unistroke text entry to freehand gesture interfaces. In *Proceedings of the 2011 Annual Conference on Human Factors in Computing Systems*. ACM, 2473–2476.

Gregorio Palmas, Myroslav Bachynskyi, Antti Oulasvirta, Hans-Peter Seidel, and Tino Weinkauf. 2014. Movexp: A versatile visualization tool for human-computer interaction studies with 3D performance and biomechanical data. *IEEE Transactions on Visualization and Computer Graphics* PP, 99 (2014), 1–1. DOI:http://dx.doi.org/10.1109/TVCG.2014.2346311

Réjean Plamondon and Adel M. Alimi. 1997. Speed/accuracy trade-offs in target-directed movements. *Behavioral and Brain Sciences* 20, 2 (1997), 279–303.

John Rasmussen, Vit Vondrak, Michael Damsgaard, Mark De Zee, Søren T. Christensen, and Zdenek Dostal. 2002. The anybody project–computer analysis of the human body. *Biomechanics of Man* (2002), 270–274.

Marta S. Santos, Vera Moniz-Pereira, Andre Lourenco, Ana Fred, and Antonio P. Veloso. 2014. Relevant elderly gait features for functional fitness level grouping. In *Proceedings of the International Conference on Physiological Computing Systems*. SCITEPRESS, 153–160.

Richard A. Schmidt, Howard Zelaznik, Brian Hawkins, James S. Frank, and John T. Quinn Jr. 1979. Motor-output variability: A theory for the accuracy of rapid motor acts. *Psychological Review* 86, 5 (1979), 415.

Garth Shoemaker, Leah Findlater, Jessica Q. Dawson, and Kellogg S. Booth. 2009. Mid-air text input techniques for very large wall displays. In *Proceedings of Graphics Interface 2009*. Canadian Information Processing Society, 231–238.

Jeff Sinclair, Philip Hingston, and Martin Masek. 2007. Considerations for the design of exergames. In *Proceedings of the 5th International Conference on Computer Graphics and Interactive Techniques in Australia and Southeast Asia (GRAPHITE'07)*. ACM, New York, NY, USA, 289–295. DOI:http://dx.doi.org/10.1145/1321261.1321313

John F. Soechting, Christopher A. Buneo, Uta Herrmann, and Martha Flanders. 1995. Moving effortlessly in three dimensions: Does Donders' law apply to arm movement? *The Journal of Neuroscience* 15, 9 (1995), 6271–6280.

Darryl G. Thelen, Frank C. Anderson, and Scott L. Delp. 2003. Generating dynamic simulations of movement using computed muscle control. *Journal of Biomechanics* 36, 3 (2003), 321–328.

Emanuel Todorov and Michael I. Jordan. 1998. Smoothness maximization along a predefined path accurately predicts the speed profiles of complex arm movements. *Journal of Neurophysiology* 80, 2 (1998), 696–714.

Matthew C. Tresch, Philippe Saltiel, and Emilio Bizzi. 1999. The construction of movement by the spinal cord. *Nature Neuroscience* 2, 2 (1999), 162–167.

Matthieu B. Trudeau, Tawan Udtamadilok, Amy K. Karlson, and Jack T. Dennerlein. 2012a. Thumb motor performance varies by movement orientation, direction, and device size during single-handed mobile phone use. *Human Factors: The Journal of the Human Factors and Ergonomics Society* 54, 1 (2012), 52–59.

Matthieu B. Trudeau, Justin G. Young, Devin L. Jindrich, and Jack T. Dennerlein. 2012b. Thumb motor performance varies with thumb and wrist posture during single-handed mobile phone use. *Journal of Biomechanics* 45, 14 (2012), 2349–2354. DOI:http://dx.doi.org/10.1016/j.jbiomech.2012.07.012

Yoji Uno, Mitsuo Kawato, and Ryoji Suzuki. 1989. Formation and control of optimal trajectory in human multijoint arm movement. *Biological Cybernetics* 61, 2 (1989), 89–101.

Anita N. Vasavada, Siping Li, and Scott L. Delp. 1998. Influence of muscle morphometry and moment arms on the moment-generating capacity of human neck muscles. *Spine* 23 (1998), 412–422.

Antonio Veloso, G. Esteves, Samuel Silva, Carlos Ferreira, and F. Brandão. 2006. Biomechanics modeling of human musculoskeletal system using Adams multibody dynamics package. In *Proceedings of the 24th IASTED International Conference on Biomedical Engineering (BioMed'06)*. ACTA Press, Anaheim, CA, 401–407. http://dl.acm.org/citation.cfm?id=1166506.1166577

Nicolas Vignais, David M. Cocchiarella, Aaron M. Kociolek, and Peter J. Keir. 2013. Dynamic assessment of finger joint loads using kinetic and kinematic measurements. In *Proceedings of the 2nd International Digital Human Modeling Symposium*.

Daniel Vogel and Ravin Balakrishnan. 2005. Distant freehand pointing and clicking on very large, high resolution displays. In *Proceedings of the 18th Annual ACM Symposium on User Interface Software and Technology (UIST'05)*. ACM, New York, NY, USA, 33–42. DOI:http://dx.doi.org/10.1145/1095034.1095041

Wytse J. Wadman, Jan J. Denier van der Gon, Reint H. Geuze, and C. R. Mol. 1979. Control of fast goal-directed arm movements. *Journal of Human Movement Studies* 5 (1979), 3–17.

Joe H. Ward Jr. 1963. Hierarchical grouping to optimize an objective function. *Journal of the American Statistical Association* 58, 301 (1963), 236–244.

Alan Traviss Welford. 1968. *Fundamentals of Skill*. Methuen.

Thomas G. Whisenand and Henry H. Emurian. 1999. Analysis of cursor movements with a mouse. *Computers in Human Behavior* 15, 1 (1999), 85–103.

Margaret M. Wierzbicka, Allen W. Wiegner, and Bhagwan T. Shahani. 1986. Role of agonist and antagonist muscles in fast arm movements in man. *Experimental Brain Research* 63, 2 (1986), 331–340.

Christian Winkler, Ken Pfeuffer, and Enrico Rukzio. 2012. Investigating mid-air pointing interaction for projector phones. In *Proceedings of the 2012 ACM International Conference on Interactive Tabletops and Surfaces (ITS'12)*. ACM, New York, NY, 85–94. DOI:http://dx.doi.org/10.1145/2396636.2396650

Jacob O. Wobbrock, Meredith Ringel Morris, and Andrew D. Wilson. 2009. User-defined gestures for surface computing. In *Proceedings of the SIGCHI Conference on Human Factors in Computing Systems (CHI'09)*. ACM, New York, NY, 1083–1092. DOI:http://dx.doi.org/10.1145/1518701.1518866

Received December 2013; revised August 2014; accepted September 2014